Separation Science and Technology
Publication details, including instructions for authors and subscription information:
http://www.informaworld.com/smpp/title~content=t713708471

Simulation of a Fractionated Vacuum Swing Adsorption Process for Air Separation

Cheng-Tung Chou; Dou-Ming Ju; Shih-Chang Chang

To cite this Article Chou, Cheng-Tung , Ju, Dou-Ming and Chang, Shih-Chang(1998) 'Simulation of a Fractionated Vacuum Swing Adsorption Process for Air Separation', Separation Science and Technology, 33: 13, 2059 — 2073
To link to this Article: DOI: 10.1080/01496399808545046
URL: http://dx.doi.org/10.1080/01496399808545046

SEPARATION SCIENCE AND TECHNOLOGY, 33(13), pp. 2059–2073, 1998

Simulation of a Fractionated Vacuum Swing Adsorption Process for Air Separation

---

CHENG-TUNG CHOU,* DOU-MING JU, and SHIH-CHANG CHANG
DEPARTMENT OF CHEMICAL ENGINEERING
NATIONAL CENTRAL UNIVERSITY
CHUNG-LI 32054, TAIWAN, REPUBLIC OF CHINA

ABSTRACT

A fractionated vacuum swing adsorption process previously proposed in the literature that simultaneously produces a 98% nitrogen-enriched gas and a 90% oxygen-enriched gas from ambient air is studied by simulation. This process utilizes CaX zeolite as the major adsorbent and alumina as the desiccant packed at the feed air end. In the isothermal simulation the feed air is considered to be a ternary mixture of nitrogen, oxygen, and water vapor, and the dynamic behavior of the adsorption bed and the effects of air humidity are studied.

INTRODUCTION

Pressure swing adsorption (PSA) plays an important role in the drying, separation, and purification of gases. Based on the differences in equilibrium adsorption amounts (such as the air–5A zeolite system) or on the differences in kinetic rates (such as the air–carbon molecular sieve system), the PSA process is able to achieve separation of a gas mixture through a cyclic pressure change. Among the many applications of PSA processes, the production of oxygen- and nitrogen-enriched gases from ambient air is an important one. However, almost all the PSA processes produce only oxygen- or nitrogen-enriched gases; the reason is mentioned below.

Because the void space in the adsorber is large and the composition of gas contained in the voids in the saturated bed is the same as the feed mixture,

---

* To whom correspondence should be addressed.

www.dekker.com

the total concentration of the strong adsorptive in the bed (in the voids plus the adsorbate) is not high. Therefore, the released vent gas which has only a relatively low concentration of strong adsorptive is discarded. In such a process there is only one product stream produced during the feed step.

An Air Products vacuum swing adsorption (VSA) process resolved such difficulty. Simultaneous production of oxygen- and nitrogen-enriched product gases was achieved by introducing a nitrogen-rinse step after the air adsorption step (9). The coadsorbed oxygen remaining in the adsorber at the end of the air adsorption step was displaced by nearly pure nitrogen flowing through the adsorber during the nitrogen-rinse step. In the next evacuation step, high purity (99+%) nitrogen was withdrawn as product and a part of it was used later as the nitrogen-rinse gas.

Chou et al. (5) utilized the idea of complementary pressure swing adsorption of Knaebel (7, 8) and proposed a four-bed process to separate air into oxygen- and nitrogen-enriched products. The principle of a complementary PSA process is to use different but complementary adsorbents; in other words, the strongly adsorbed component on one adsorbent is weakly adsorbed on the other.

Recently Air Products developed a fractionated vacuum swing adsorption (FVSA) process which simultaneously produces a 98+% nitrogen-enriched gas and an 80–90% oxygen-enriched gas from ambient air (10). This process demands the use of a zeolite which exhibits a high nitrogen adsorption capacity and selectivity from air. CaX zeolite was used for this purpose. Because water vapor is strongly adsorbed on zeolite, water vapor in air has to be removed before air is in contact with zeolite. Usually the removal of water vapor is pretreated before air flows into the adsorption bed. To the best of our knowledge, in previous simulation studies of PSA air separation only the adsorption of oxygen and nitrogen (sometimes also the adsorption of argon) was considered. Nevertheless, in the FVSA process a desiccant alumina was packed in front of the CaX zeolite to save the need for water removal pretreatment. For this FVSA process, apparently the strong adsorption of water, which may cause numerical stiffness, has to be considered in simulation. The purpose of this study is to include the numerical stiffness of water in air–PSA simulation for the first time, and to utilize this simulation program to study the influence of inlet air humidity on the performance of the FVSA process.

FVSA PROCESS

The FVSA process studied is a dual-bed four-step process which simultaneously produces concentrated oxygen and nitrogen with ambient air as the feed. Each bed operates independently, and the oxygen- and nitrogen-enriched gases are delivered to an oxygen tank and a nitrogen tank, respectively, from

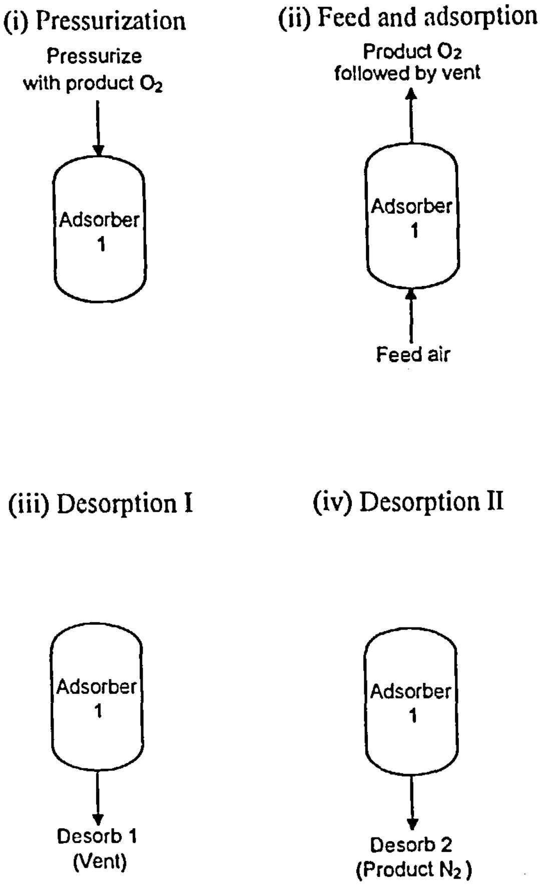

FIG. 1 Steps of FVSA for air separation.

which the products are withdrawn. Desiccant alumina and adsorbent CaX zeolite are sectionally packed in the bed with alumina near the feed end. Taking Bed 1 as an example, the four steps are shown in Fig. 1.

(i) Pressurization with oxygen-enriched product
0–15 seconds: Bed 1 is pressurized with the oxygen-enriched product from the oxygen tank.

(ii) Feed and adsorption
15–30 seconds: Bed 1 is fed by high-pressure air and produces oxygen-enriched gas.

30–45 seconds: Bed 1 is fed by high-pressure air and vents gas from the product end.

(iii) Desorption I

45–60 seconds: Bed 1 is depressurized and vents gas.

(iv) Desorption II

60–120 seconds: Bed 1 is depressurized and produces nitrogen-enriched product.

The corresponding status of Bed 2 is:

0–60 seconds: At desorption step II.
60–75 seconds: At pressurization step.
75–90 seconds: Bed 2 is fed by high-pressure air and produces oxygen-enriched gas.
90–105 seconds: Bed 2 is fed by high-pressure air and vents gas from the product end.
105–120 seconds: At desorption step I.

MATHEMATICAL MODEL

For the air system studied, the following assumptions are assumed.

1. The adsorption of nitrogen and oxygen on CaX zeolite are very fast so we can use an equilibrium model to describe it, i.e., the adsorbate concentrations in the gas phase and the solid phase reach equilibrium instantaneously at the same cross section of the adsorption bed. To simplify the calculation, we make the same assumption for water. The adsorption amount of nitrogen and oxygen on alumina can be neglected.
2. The pressure drop through the adsorption bed can be neglected.
3. The ideal gas law can be applied.
4. Isothermal operation is assumed.
5. There are no radial thermal and concentration gradients.
6. Argon and oxygen are taken as the same component in simulation because the mole fraction of argon in air is small (about 1%) and the adsorption property of argon is similar to that of oxygen (4).

Subject to these assumptions, the governing equations describing the dynamic behaviors of the PSA process are: For the overall material balance:

$$-\frac{\partial q}{\partial z} = \frac{\epsilon A}{R}\frac{\partial (P/T)}{\partial t} + (1 - \epsilon)A\sum_{i=1}^{n}\frac{\partial n_i}{\partial t} \tag{1}$$

and the material balance of component i:

$$\frac{\partial}{\partial z}\left(\frac{\epsilon APD_{\mathrm{ax}i}}{RT}\frac{\partial y_i}{\partial z}\right) - \frac{\partial(y_i q)}{\partial z} = \frac{\epsilon A}{R}\frac{\partial}{\partial t}\left(\frac{y_i P}{T}\right) + (1-\epsilon)A\frac{\partial n_i}{\partial t}, \quad i = 1, \ldots, n-1 \tag{2}$$

Axial dispersion coefficients can be calculated from the equation mentioned in Wen and Fan (11). The dependence of molecular diffusivity on pressure can be described by the Chapman–Enskog equation (1). The adsorption equilibrium isotherm used for the adsorption on CaX zeolite is the extended Langmuir equation:

$$n_i^* = \frac{\rho_s a_i y_i p}{1 + \sum_{i=1}^{n} b_i y_i p} \tag{3}$$

and that for water adsorption on alumina is the BET equation:

$$n_i^* = \frac{\rho_s c_i q_i p_i^r}{(1 - p_i^r)(1 - p_i^r + c_i p_i^r)} \tag{4}$$

where $p_i^r = p_i/p_i^{\mathrm{sat}}$ and n_i^* is the equilibrium adsorption amount of component i.

The initial condition is a bed saturated with air containing 10^{-6} mole fraction of water at 1 atm and 303.14 K. The boundary conditions are:

1. At the inlet end

$$y_i = y_{i,\mathrm{in}}$$

2. At the outlet and closed end

$$\partial y_i/\partial z = 0$$

3. Between the two adsorbents

$$\left.\left(y_i q - \frac{\epsilon APD_{\mathrm{ax}i}}{RT}\frac{\partial y_i}{\partial z}\right)\right|_{+} = \left.\left(y_i q - \frac{\epsilon APD_{\mathrm{ax}i}}{RT}\frac{\partial y_i}{\partial z}\right)\right|_{-}$$

Because of the numerical difficulty caused by the large oxygen concentration difference between the feed air and the gas inside the bed, we set the feed concentration to be smoothed as

$$y_i = y_{i,\mathrm{bed}} + (y_{i,\mathrm{in}} - y_{i,\mathrm{bed}})(1 - e^{-4t^2})$$

We applied the method of lines with adaptive grid points combined with an estimation of the spatial derivatives by cubic spline/finite difference to discretize the partial differential equations (PDEs) into a set of ordinary differential equations (ODEs), then the set of ODEs was integrated with respect

TABLE 1
The Parameters of Adsorber and Adsorbent Used in Simulation

Total bed length (*L*)	182.88 cm
Inner diameter of bed (*D*)	5.08 cm
CaX zeolite porosity (ϵ)	0.69
CaX zeolite bulk density (ρ_b)	0.64 g/cm^3
CaX zeolite diameter (d_p)	0.158 cm
Alumina porosity (ϵ)	0.69
Alumina bulk density (ρ_b)	0.75 g/cm^3
Alumina diameter (d_p)	0.158 cm
CaX zeolite Langmuir isotherm parameters:	
$a(O_2)$	2.509 × 10^{-4} mol/g-atm (10)
$a(N_2)$	2.551 × 10^{-3} mol/g-atm (10)
$a(H_2O)$	2.6701 × 10^{1} mol/g-atm (6)
$b(O_2)$	2.240 × 10^{-1} l/atm (10)
$b(N_2)$	2.278 l/atm (10)
$b(H_2O)$	1.2971 × 10^{3} l/atm (6)
Alumina BET isotherm parameters:	
$q(H_2O)$	2.283 × 10^{-3} mol/g (2)
$c(H_2O)$	2.208 × 10^{1} (2)

to time by using the subroutine LSODE of the package ODEPACK to obtain the dynamic solution of this system. The calculations were repeated until the cyclic steady-state was reached. The details of the calculating procedures can be found in Chou et al. (5) The flow rates through the valves were calculated from a valve equation (3).

RESULTS AND DISCUSSION

The parameters of the adsorber and adsorbent used in simulation and the operation conditions of FVSA process are listed in Tables 1 and 2. The calcu-

TABLE 2
Operating Conditions of FVSA Process

Feed pressure	1.1 atm
Product pressure:	
O_2	1.0 atm
N_2	0.092 atm
Vent pressure	0.37 atm
Feed temperature	303.14 K
Room temperature	303.14 K

lations took about 25 CPU seconds for each cycle, and it took about 30 cycles to reach cyclic steady-state for the FVSA process in a DEC AXP 3000/400 workstation.

Comparison with Experimental Data in the Literature

For a feed air of 60% relative humidity (2.28% H_2O, 21.38% O_2 and Ar, 76.34% N_2), Figs. 2 and 3 show the comparison between the simulation results and the experimental data of Sircar and Hanley (10). In Fig. 2 the calculated column pressure agrees very well with the experimental data whereas in Fig. 3 the calculated nitrogen product purity is closer to the experimental value as the fraction desorbed nears 1, but there is some discrepancy between the calculated and experimental values while the fraction desorbed is near 0. Because the gas released during the desorption steps is vented through the feed-air end of the adsorber, the first gas released should have a composition similar to the feed air, i.e., when the fraction desorbed is near 0, the composition of the vented nitrogen product should be near that of air.

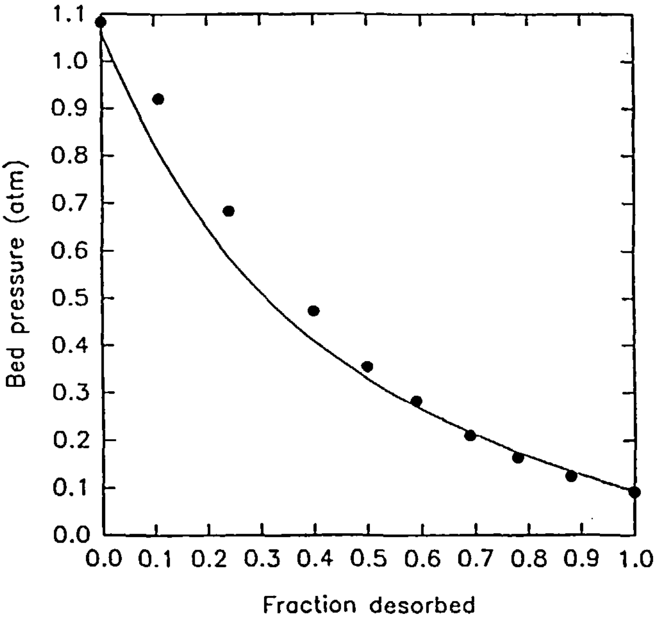

FIG. 2 Bed pressure vs fraction desorbed. (●) Experimental data of Sircar and Hanley (10). (——) Simulation results.

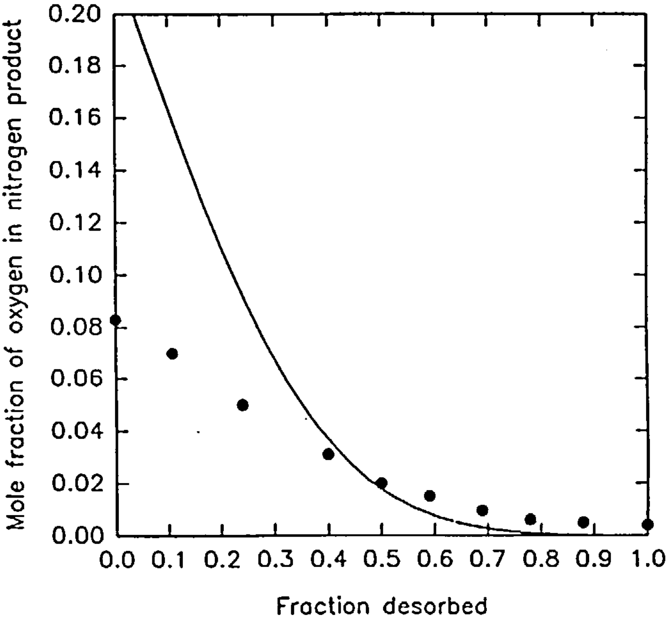

FIG. 3 Mole fraction of oxygen in nitrogen product vs fraction desorbed. Symbols as in Fig. 2.

TABLE 3
Comparison between Experimental Data (10) and Simulation Results[a]

	Purity (%)	Recovery (%)	Capacity (mol/kg-cycle)
	Oxygen Product		
Experimental data	90.0	24.2	0.04
Simulation	91.58	24.88	0.052
	Nitrogen Product		
Experimental data	98.0	42.6	0.25
Simulation	94.20	43.04	0.336

[a] Relative humidity of inlet air in simulation = 60%.

This is why simulation predicts an oxygen mole fraction near 0.21 when the fraction desorbed is near 0 in Fig. 3.

In the initial desorbing stage the simulation predicts a nitrogen product purity similar to air, whereas the measured nitrogen purity of Sircar and Hanley (10) is near 92%. Such a discrepancy disappears when the fraction desorbed is larger than 0.4. Inasmuch as the nitrogen product is collected in the process while the fraction desorbed is greater than 0.35 (the initially desorbed gas is vented in desorption step I), the calculated and measured average nitrogen product purities are close, as shown in Table 3.

The product recovery is defined as the ratio of the amount of product in the product stream over that in the feed stream, and the adsorbent capacity is defined as the amount of product in the product stream per cycle per unit

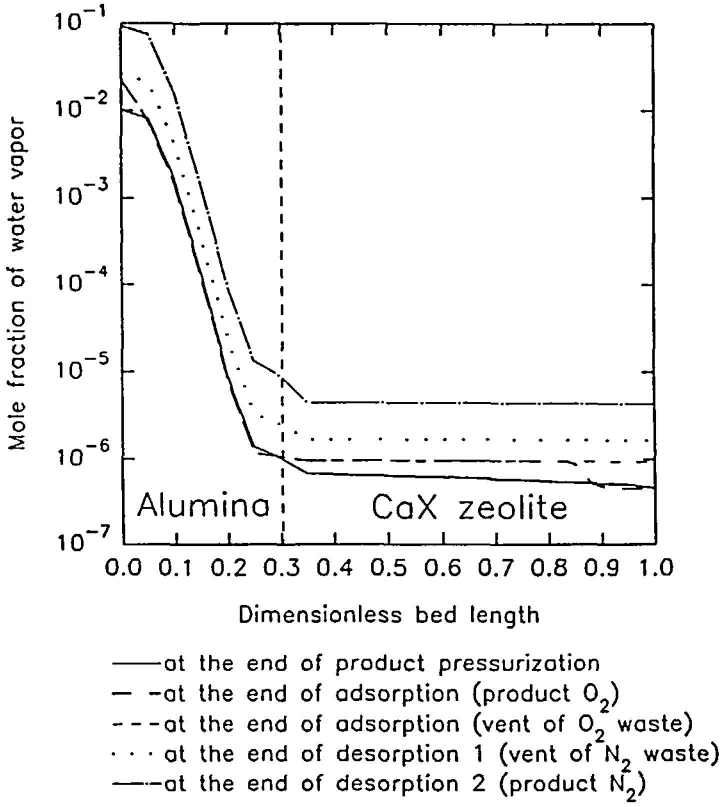

FIG. 4 Concentration profiles of water vapor at the end of each step.

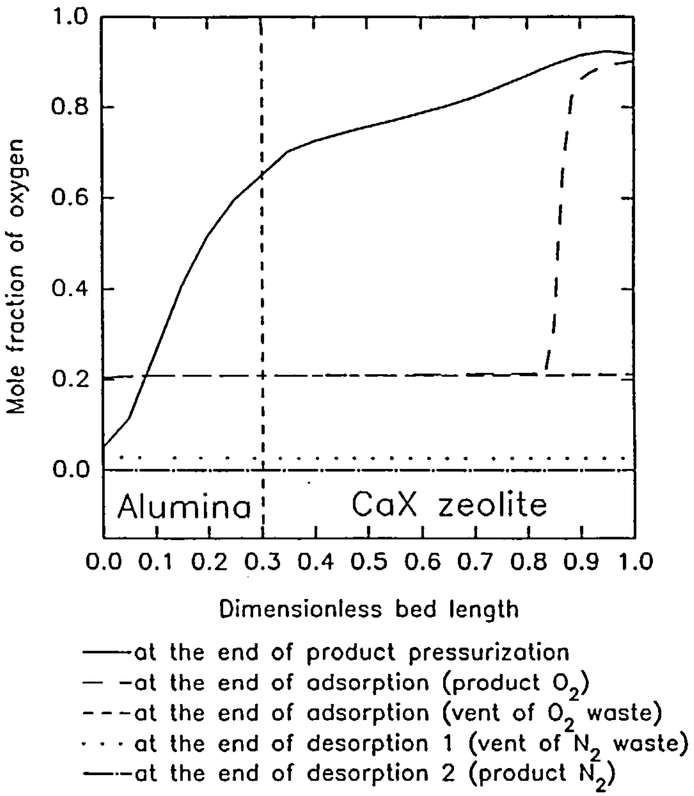

FIG. 5 Concentration profiles of oxygen at the end of each step.

weight of adsorbent. Table 3 shows good agreement in product purity and recovery between the simulation and experiments, but higher values of calculated adsorbent capacity than in the experimental data. The difference of adsorbent capacity between the simulation and experiment data may be due to the assumption of isothermal operation. Figures 4 to 6 show the calculated bed concentration profile for each component at the end of each step. As shown in Fig. 4, the alumina packed in the feed end of the bed is capable of removing the water vapor in the feed air, and the mole fraction of water in the CaX zeolite section is always less than 10^{-5}. According to Fig. 5, pressurization of the bed with the oxygen product makes the oxygen concentration profile increase a lot, which contributes to a better oxygen product purity. Figure 6 shows that during desorption step II (nitrogen product) the

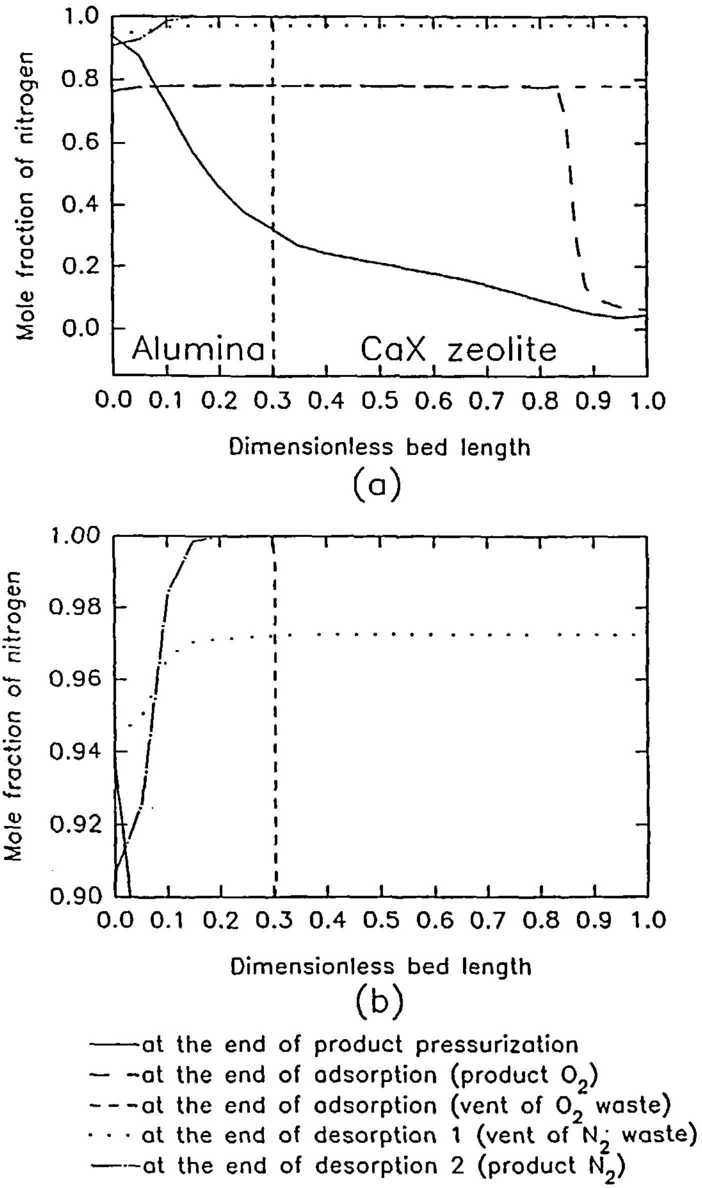

FIG. 6 Concentration profiles of nitrogen at the end of each step: (b) is the magnification of (a) in the high-purity region.

desorbed nitrogen makes the gas inside the bed nearly all nitrogen except for the region near the feed end. The not-so-high nitrogen purity near the feed end of the bed is due to the desorbed water in the alumina section which lowers the mole fraction of nitrogen.

Effect of Feed Air Humidity

The effect of the humidity of the feed air was also studied by simulation. As the relative humidity of air increases, the recovery, capacity, and purity of the oxygen product slightly decrease, as shown in Fig. 7, but the recovery, capacity, and purity of the nitrogen product decrease a lot, as shown in Fig. 8. As the relative humidity increases from 0 to 100%, the purity of nitrogen product decreases from 99+ to 91%. As the relative humidity of air increases, more water is apparently adsorbed on alumina, and therefore more water is desorbed from alumina during the desorption step, which in turn decreases the quality of the nitrogen product.

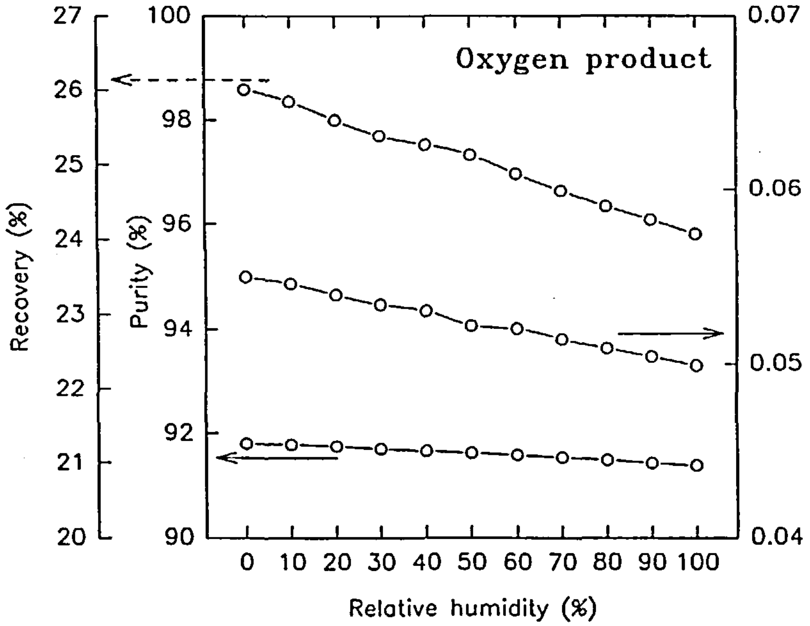

FIG. 7 Effect of feed air humidity on oxygen product.

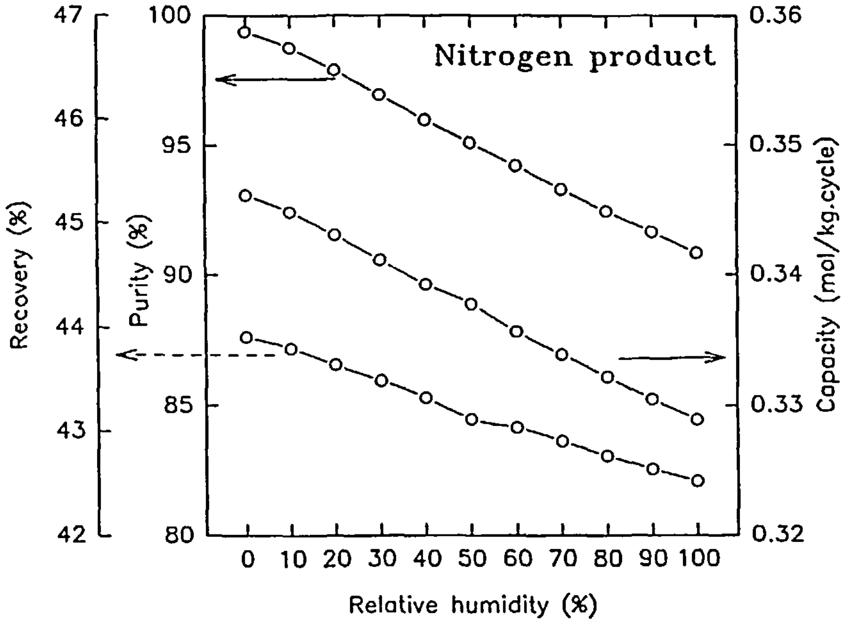

FIG. 8 Effect of feed air humidity on nitrogen product.

CONCLUSION

This study dynamically simulates a dual-bed four-step fractionated vacuum swing adsorption (FVSA) process with desiccant alumina and adsorbent CaX zeolite packed in the same bed which simultaneously produces oxygen- and nitrogen-enriched gases. Humidity of the feed air is unfavorable for this system. The alumina section does dry the feed air, but the desorbed water in the vacuum desorption step decreases the purity of the nitrogen product.

NOTATION

a_i	parameter in Langmuir isotherm (mol/g-atm)
A	cross-section area of the bed (cm^2)
b_i	parameter in Langmuir isotherm (atm^{-1})
c_i	parameter in BET equation (dimensionless)
D	diameter of packed bed (cm)
D_{ax}	axial dispersion coefficient (cm^2/s)
D_{m}	molecular diffusivity (cm^2/s)

L	length of packing (cm)
n	number of components
n_i	adsorption amount of component i per unit volume of adsorbent (mol/cm^3)
P	pressure (atm)
q	molar flow rate (mol/s)
q_i	parameter in BET equation (mol/g)
R	gas constant (82.06 atm-cm^3/mol-K)
T	temperature (K)
t	time (s)
y_i	mole fraction of component i in gas phase (dimensionless)
z	axial distance along adsorption bed (cm)

Greek Letters

ϵ	void fraction of packed bed (dimensionless)
ρ_b	bulk density of adsorbent (g/cm^3)
ρ_s	adsorbent particle density (g/cm^3)

Superscript

*	adsorption equilibrium state

Subscripts

bed	bed condition at inlet end
i	component i
in	inlet stream
0	reference state

ACKNOWLEDGMENT

This work was supported by the National Science Council of the Republic of China under Grant NSC84-2214-E008-003.

REFERENCES

1. R. B. Bird, W. E. Stewart, and E. N. Lightfoot, *Transport Phenomena*, Wiley, New York, NY, 1960, pp. 196–200.
2. D. W. Breck, *Zeolite Molecular Sieves: Structure, Chemistry and Use*, Wiley, New York, NY, 1974, p. 613.
3. C. T. Chou and W. C. Huang, "Incorporation of a Valve Equation into the Simulation of a Pressure Swing Adsorption Process," *Chem. Eng. Sci.*, *48*(1), 75–84 (1994).

4. C. T. Chou and L. H. Chen, "Ternary Component Simulation of a Pressure Swing Adsorption Process for Air Separation," *J. Chin. Inst., Chem. Eng.*, *25*(6), 361–366 (1994).
5. C. T. Chou, C. L. Wu, and A. S. T. Chiang, "A Complementary Pressure Swing Adsorption Process Configuration for Air Separation," *Sep. Technol.*, *4*, 93–103 (1994).
6. R. Desai, M. Hussain, and D. M. Ruthven, "Adsorption of Water Vapour on Activated Alumina. I. Equilibrium Behaviour," *Can. J. Chem. Eng.*, *70*, 699–706 (1992).
7. K. S. Knaebel, "Analysis of Complementary Pressure Swing Adsorption," in *Fundamentals of Adsorption* (A. L. Myers and G. Belfort, Eds.), Engineering Foundation, New York, NY, 1984, p. 273.
8. K. S. Knaebel, US Patent 4,744,803 (1988).
9. S. Sircar and J. W. Zondlo, US Patent 4,013,429 (1977).
10. S. Sircar and B. F. Hanley, "Fractionated Vacuum Swing Adsorption Process for Air Separation," *Sep. Sci. Technol.*, *28*(17), 2553–2565 (1993).
11. C. Y. Wen and L. T. Fan, *Models for Flow Systems and Chemical Reactors*, Dekker, New York, NY, 1975, pp. 169–171.

Received by editor September 2, 1997
Revision received January 1998